Mg-rich dumortierite in cordierite–orthoamphibole-bearing rocks from the high-grade Bamble Sector, south Norway

DIEDERIK VISSER AND ANTONY SENIOR

Department of Petrology and Experimental Petrology, Institute of Earth Sciences, University of Utrecht, P.O. Box 80.021, 3508 TA Utrecht, The Netherlands

Abstract

Dumortierite is described from several occurrences of cordierite–orthoamphibole-bearing rocks in the upper-amphibolite facies area of the Bamble Sector, south Norway. Dumortierite occurs with chlorite, muscovite and quartz in late M_4 alteration zones or aggregates after M_3, peak-metamorphic cordierite and garnet and early M_4 vein-cordierite, and intergrown with or replacing orthoamphibole. Late M_4 *P–T* conditions, which are interpreted as conditions of dumortierite formation, are estimated from the associated late M_4 kyanite–andalusite–chlorite–quartz assemblage and Mg–Fe exchange geothermometry to be 500 ± 50 °C and 3–4 kbar. Retrogression of M_3 mineral assemblages is initiated by influx of fluids with X_{CO_2} of 0.3–0.4 during early M_4 followed by more water-rich fluids during late M_4. Late M_4 fluids may show local variations in alkalis and boron. The dumortierites are the most Mg-rich (2.23–3.42 wt.% MgO) ever reported, and contain 0.00–2.05 wt.% TiO_2, 0.00–1.08 wt.% Fe_2O_3, 29.62–32.42 wt.% SiO_2 and 55.20–59.71 wt.% Al_2O_3. Al is the most likely substituent for Si, which shows a minor deficiency at the tetrahedral sites in most dumortierites. The major variations in the mineral chemistry can be described by the coupled substitutions $Mg + Ti = 2Al^{VI}$, $3Mg = 2Al^{VI}$ and possibly $Mg + H = Al^{VI}$. Favoured by low f_{O_2} prevailing conditions a significant part of total iron in dumortierites at one locality is present as Fe^{2+} giving evidence for the $Fe^{2+} + Si^{IV} = Al^{IV} + Al^{VI}$ tschermakite substitution. $FeMg_{-1}$ substitution is considered to be limited. Ti-rich dumortierites coexist with rutile, ilmenite or titaniferous magnetite. The development of dumortierite from orthoamphibole correlates with an observed decrease of Al, Mg and Na and increase of Si and Fe in orthoamphibole towards dumortierite.

KEYWORDS: Bamble Sector, south Norway, cordierite, Mg-rich dumortierite, garnet, orthoamphibole.

Introduction

RECENT microscopic investigations of cordierite–orthoamphibole-bearing rocks from the Bamble Sector, south Norway, revealed several new occurrences of the relatively uncommon borosilicate dumortierite (Fig. 1). This rare mineral has already been reported from the same area by Bugge (1943) and Touret (1979). The first discovery however was questioned by Lamb (1981), who identified the blue mineral of Bugge as sapphirine.

Dumortierite is generally reported as a minor constituent in pegmatitic, aplitic, and granitic rocks (e.g. Finlay, 1907; Graham and Robertson, 1951; Huijsmans *et al.*, 1982), associated pneumatolytic–hydrothermal deposits (Kerr and Jenney, 1935; Sabzehei, 1971; Black, 1973) and regional metamorphic quartzites, argillaceous gneisses and granulites (e.g. Christophe-Michel-Lévy *et al.*, 1959; Schreyer *et al.*, 1975; Vrána, 1979; Takahata and Uchiyama, 1985; Beukes *et al.*, 1987). More than 75 years after its discovery by Gonnard (1881), the space group (*Pmcn*), unit-cell parameters and preliminary general formula for the orthorhombic dumortierite, $(Al,Fe^{3+})_7BSi_3O_{18}$, were deduced by Claringbull and Hey (1958). Its crystal structure was solved by Golovastikov (1965), confirming the space group *Pmcn* assigned by Claringbull and Hey (1958), and further refined by Moore and Araki (1978). The presence of water has undoubtedly been demon-

Mineralogical Magazine, December 1991, Vol. 55, pp. 563–577

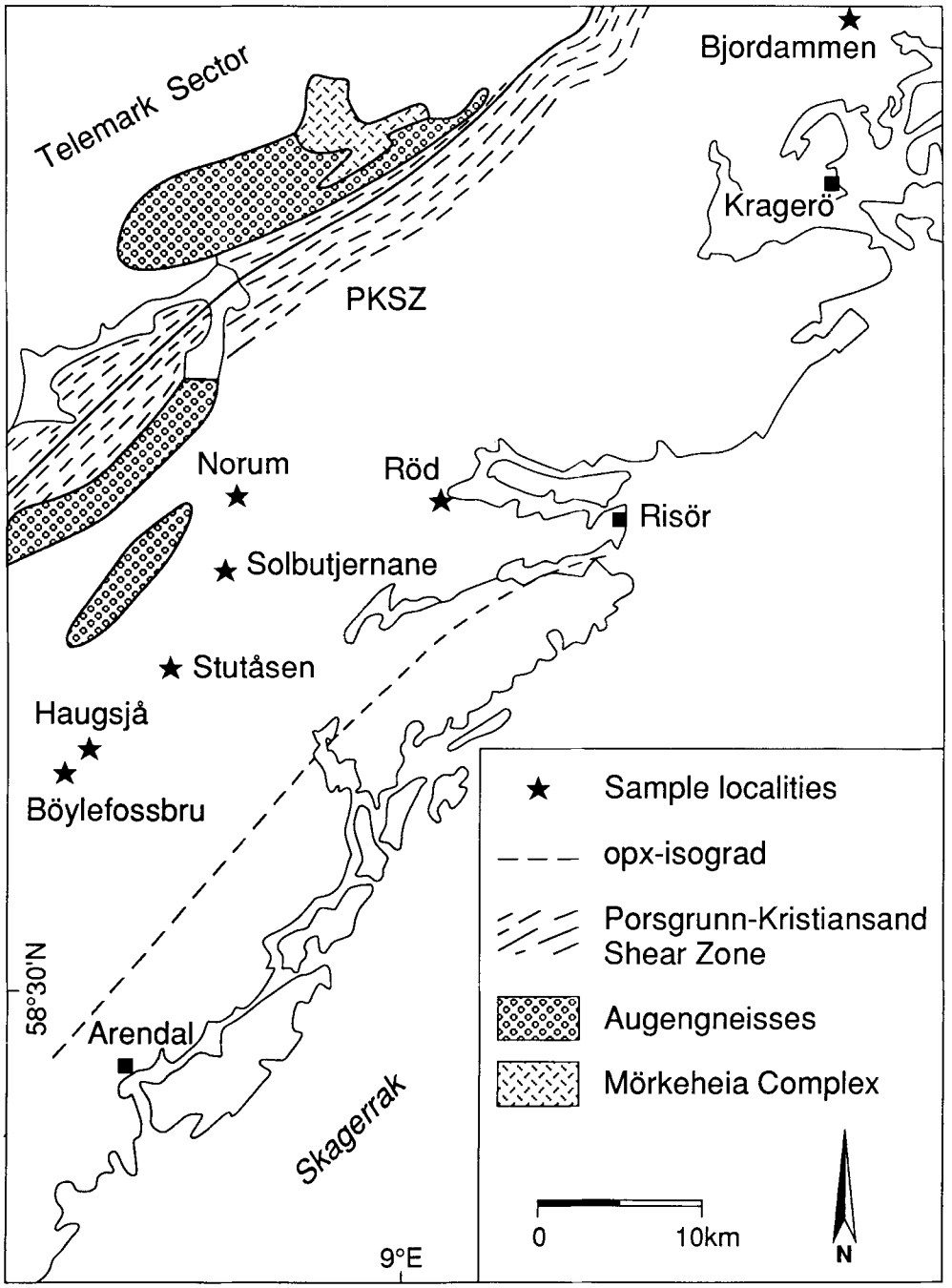

FIG. 1. Locality and simplified geological map of the central part of the Bamble Sector, south Norway. Opx-isograd after Field and Clough (1976).

strated by several studies (e.g. Moore and Araki, 1978; Alexander *et al.*, 1986; Werding and Schreyer, 1988; 1990) giving the rearranged general formula of dumortierite, $Al_{6.75}\square_{0.25}BSi_3[O_{17.25}(OH)_{0.75}]$ (after Moore and Araki, 1978). Recently Werding and Schreyer (1988, 1990) were able to synthesise dumortierite in the system Al_2O_3–B_2O_3–SiO_2–H_2O. Their experimental data show a variation of H_2O-contents.

In this paper, the occurrence in cordierite–orthoamphibole-bearing rocks and the Mg-rich mineral chemistry of the Bamble dumortierites will be presented and discussed. Some considerations on the *P–T* conditions of formation will be given.

Geological setting

The dumortierite-bearing cordierite–orthoamphibole rocks occur as thin layers and lenses in the upper-amphibolite facies area of the central part of the Bamble Sector (Fig. 1). The high-grade Bamble Sector was subject to two major periods of metamorphism and deformation (Starmer, 1985). Aluminous reaction textures in orthoamphibole-bearing rocks record a 'near-clockwise' prograde *P–T* trajectory (M_1–M_3) for the Kongsbergian Orogeny (1600–1500 Ma) (Visser and Senior, 1990). This prograde *P–T* path is explained as a collision scenario with magmatic addition which produced NE–SW elongated structures. Peak-metamorphic conditions (M_3) reached upper-amphibolite to granulite facies conditions of about 800 ± 60 °C and 7.3 ± 0.5 kbar (Lamb *et al.*, 1986). A long period (300 Ma) of near isobaric cooling occurred between the Kongsbergian Orogeny and the second major period of metamorphism and deformation, the Sveconorwegian (*ca.* 1200–1000 Ma) Orogeny. The tectonic effects of the Sveconorwegian Orogeny (M_4 according to Visser and Senior, 1990) in the Bamble Sector are more pronounced towards its margin with the Telemark Sector. 'Near'-isothermal uplift of the Bamble Sector, representing emplacement in the upper crust, is indicated by M_4 assemblages in cordierite–orthoamphibole-bearing rocks which include talc–kyanite–quartz (early M_4) and kyanite–andalusite–chlorite–quartz (late M_4) (Visser *et al.*, 1990). Domains with 'Kongsbergian' structures and ages as e.g. the Arendal granulite facies terrain, largely seem to have survived the effects of the Sveconorwegian Orogeny (Starmer, 1985, 1990). The Sveconorwegian Orogeny, an event of extensive but channelled fluid activity associated with the formation of pegmatites, granite, albitites and quartz-veins, regionally reached greenschist to mid-amphibolite facies conditions. Locally upper-amphibolite to low-granulite facies contact-metamorphic conditions were recorded around augengneiss bodies (Nijland and Senior, 1991).

Petrography

Dumortierite was found as a minor constituent at seven localities of cordierite–orthoamphibole-bearing rock-types and associated quartz–cordierite veins in the upper-amphibole facies area. At each locality, the dumortierite grains are so scarce and small that they were found in only about one out of five to ten thin sections. In Table 1, the location and metamorphic assemblages of the dumortierite-bearing samples are listed.

Dumortierites in all samples have a secondary origin. Three types can be distinguished (see Table 1):

I. Dumortierite intergrown with retrograde alteration products of cordierite (samples AK 034, DV 034, DV 249, MA 822, RV 070, TN 087),
II. Dumortierite intergrown with retrograde alteration products along cracks in garnet (samples AK 036, DV 030, MA 780),
III. Dumortierite intergrown with orthoamphibole or replacing orthoamphibole (samples DV 183, MA 780),

The first type of dumortierite occurs in two generations of cordierite, namely a primary cordierite of the peak metamorphic M_3-assemblage and a secondary cordierite in probably early-M_4 quartz–cordierite veins which cut across M_3-assemblages. Both generations of cordierite locally show severe pinitisation and in some grains the typical coarse-grained late-M_4 assemblage consisting of kyanite–(± andalusite)–chlorite–quartz developed. The euhedral to subhedral dumortierite grains occur at the margin of the alteration aggregates composed of chlorite + quartz + pinite ± kyanite ± andalusite (Figs. 2 and 3). Intergrowth of dumortierite with kyanite or andalusite has not been observed. Type I dumortierite occasionally is in contact with titaniferous magnetite (C. Maijer, unpublished data). The dumortierite grains normally are very small (50–175 μm in length) but dumortierite in sample AK 034 measures up to 350 μm in length (Fig. 3). Besides the red pleochroism (X = red, Y = Z = colourless), the type I dumortierites sometimes display a faint purple–blue pleochroism in the centre of the grains. Large euhedral, optically unzoned, pale yellow to light brown–green tourmaline grains up to 700–900 μm accompany quartz and cordierite in samples MA 822, AK 034

Table 1. The location and mineral assemblage in selected samples. Map references are from maps prepared by Norges Geografiske Oppmåling, Series M711, sheets 1612 II-III and 1712 IV.

	Locality		Sample	Minerals
1	Böylefossbru	4831-64966	DV 030	Qtz, Grt, Oam, Bt, Crd (M_3), Ap, Rt, St, (Chl, Ms, Dum II)
			DV 034	Qtz, Crd (M_4), Ap, (Chl, Ky, And, Ms, Tur, Dum I)
			DV 249	Qtz, Oam, Crd (M_3), Bt, Rt, Ap, (Chl, Ms, Ky, Dum I)
2	Haugsjå	4844-64968	TN 087	Qtz, Oam, Grt, Crd (M_3), Bt, Rt, Opq, (Ky, Ms. Chl, Dum I, Cc)
3	Stutåsen	4886-65009	DV 183	Qtz, Oam, Bt, Crd (M_3), Rt, Grt, (Ms, Chl, Dum III)
4	Solbutjernane	4915-65059	RV 070	Qtz, Crd (M_4), Bt, Rt, Opq, (Tlc, Chl, Tur, Dum I, Cc, Preh)
5	Norum	4921-65098	AK 034	Qtz, Grt, Tur, Bt, Rt, Opq, Crd (M_3), (Rt, Ms, Chl, Tur, Ky, And, Dum I)
			AK 036	Qtz, Oam, Grt, Crd (M_4), Bt, Tur, Opq, Rt, (Ky, And, Ms, Chl, Cc, Tlc, Dum II)
6	Röd	5030-65096	MA 780	Grt, Bt, Crd (M_3), Oam, Qtz, Ap, Tur, Krn, Gr, Opq, Rt, Ilm, (Dum II, Dum II, Chl, Ms)
7	Bjordammen	5245-65342	MA 822	Qtz, Bt, Crd (M_4), Ap, Tur, Mag, (Chl, Ky, And, Ms, Tur, Dum I)

Mineral abbreviations after Kretz (1983)
Dumortierite type I, II or III (Dum I, Dum II and Dum III) (see text), Muscovite/pinite (Ms), Opaque (Opq). Square brackets indicate secondary minerals. (M_3, M_4) - Primary M_3-cordierite and early-M_4 vein-cordierite.

and AK 306; smaller euhedral yellow–green tourmaline grains (up to 400 μm) occur with chlorite, quartz and Al-silicate in the centre and at the margin of the alteration aggregates of cordierite in samples DV 034, RV 070, AK 034 and MA 822. The smaller tourmalines and dumortierites never occur intergrown within the same alteration aggregate.

Type II dumortierite occurs along narrow retrograde zones or cracks in garnet blasts (Fig. 4), which may measure up to several centimetres in diameter in sample DV 030. Dumortierite commonly forms single acicular euhedral crystals (X = red, Y = Z = colourless to very pale yellow) but subparallel bundles may be present. The dumortierites in DV 030 are accompanied by euhedral large chlorites (up to 600 μm), quartz and fine grained white mica. Type II dumortierite grains may be up to 400 μm in length and 80 μm in width. Although rutile is an important minor phase no contacts with dumortierite are observed.

Type III dumortierite is situated in narrow (up to 4 mm wide) retrograde zones or cracks, along which severe pinitisation of cordierite, chloritisation of garnet, biotite and orthoamphibole occurs. Dumortierites in these zones predominantly are intergrown as irregular shaped crystals (X = red-rosa, Y = Z = colourless to pale yellow) and fibrous masses (Fig. 5) with or developed at the expense of subhedral to euhedral orthoamphibole. Rarely type III dumortierites occur as subparallel and sheave-like aggregates of euhedral crystals (X = red, Y = Z = colourless to pale yellow) intergrown with orthoamphibole along the cleavages. Individual crystals measure up to 200 μm in length. Minor quartz, ilmenite and rutile accompany the dumortierite grains. Euhedral type II dumortierite may be present in sample MA 780 (Table 1).

Colourless kornerupine and yellow–brown tourmaline occur together with dumortierite in sample MA 780. Kornerupine is present as euhedral to subhedral grains intergrown with garnet, quartz and graphite and with orthoamphibole along the cleavage planes. Although intergrowth textures with orthoamphibole are very similar no overgrowths or intergrowths of type III dumortierite and kornerupine are observed. Retrogradation of kornerupine from kornerupine–orthoamphibole intergrowths dissected by alteration zones only produces chlorite and fine-grained white mica.

Subhedral to euhedral yellow–brown tourmaline occurs in minor amounts overgrowing biotite and as inclusion or intergrowth with M_3-cordierite, garnet and quartz. No textural relation with kornerupine or dumortierite is observed.

Common alteration products of dumortierite such as muscovite/sericite and kaolinite (Schaller, 1905; Sabzehei, 1971; Beukes *et al.*, 1987) were not observed in the investigated samples.

Mineral chemistry

Mineral analyses have been obtained using a Jeol JXA-8600 Superprobe at the University of Utrecht which operated at an acceleration potential of 15 kV, and a sample current of 10 nA. Raw data were corrected with a Tracor Northern PROZA computer program. Natural minerals and synthetic compounds were used as standards. Due to the small size of the dumortierite grains no boron or water analyses could be obtained.

Dumortierite compositions were calculated on the basis of 18 oxygens assuming one B and 0.75 OH per formula unit (after Moore and Araki, 1978). The crystal structure of dumortierite can be visualised to consist of three distinct types of chains built of AlO_6 octahedra and running parallel to the [001] direction (see Moore and Araki (1978) for graphic representation of the structure and site-notation). The first, $Al(1)O_3$ chain, is a disordered central infinite face-sharing chain linked in a pseudohexagonal fashion to six external, $3Al(2)_2$-$Al(3)_2O_{12}$ and $3Al(4)O_{12}$, octahedral chains by six isolated $2Si(1)O_4$ + $4Si(2)O_4$ tetrahedra. The second, $Al(2)_2$-$Al(3)_2O_{12}$ chain is an inversion doubled pyroxene-like edge-sharing chain. The third type is a pyroxene-like edge-shared chain doubled to an $Al(4)_4O_{12}$ chain by face-sharing. The external chains are interconnected by BO_3 triangles. X-ray site refinements of Moore and Araki (1978) and Alexander *et al.* (1986) indicate that site-occupancies of the B, Al(2), Al(3) and Si(1,2) sites converge to full occupancy (≈0.95). The Al(1) central site is only partially occupied (75 and 80% according to Moore and Araki (1978) and Alexander *et al.* (1986) respectively). Charge-balance requirements for this site involve the $3H^+ + \square^{VI} = Al^{3+VI}$ substitutional mechanism and giving the general formula $(Al_{6.75}\square_{0.25})BSi_3[O_{17.25}$-$(OH)_{0.75}]$. As postulated by Alexander *et al.* (1986) the total amount of (OH) will not only vary with the number of octahedral vacancies but also

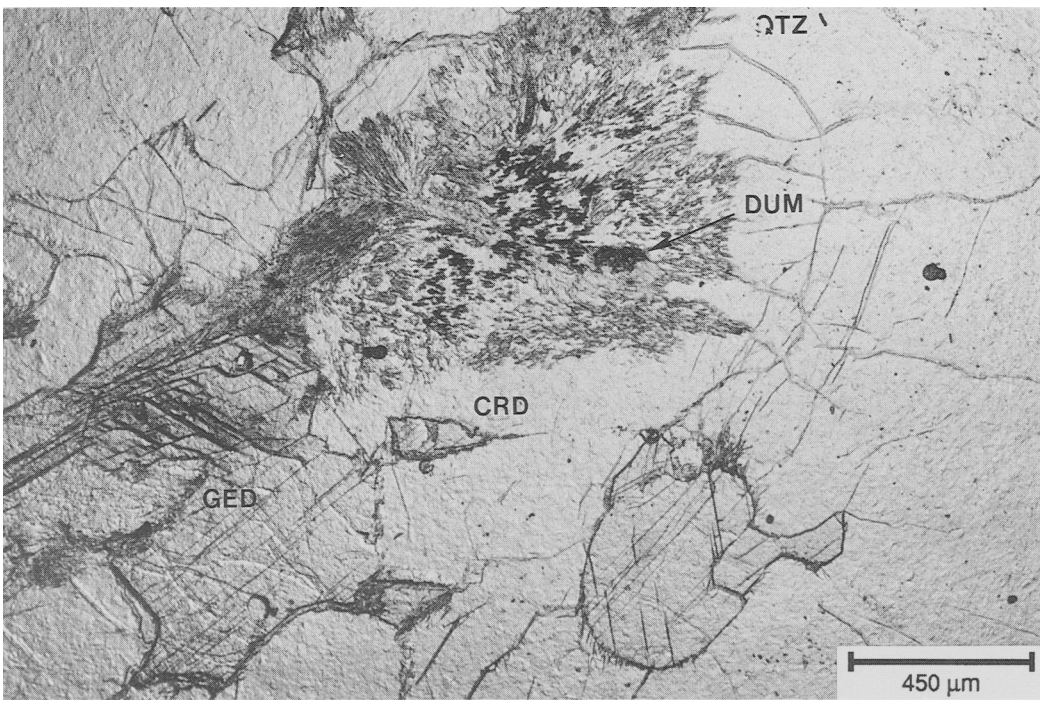

FIG. 2. Photomicrograph of an alteration aggregate in cordierite (CRD) from sample DV 249. Type I dumortierite (DUM) is intergrown with chlorite and muscovite.

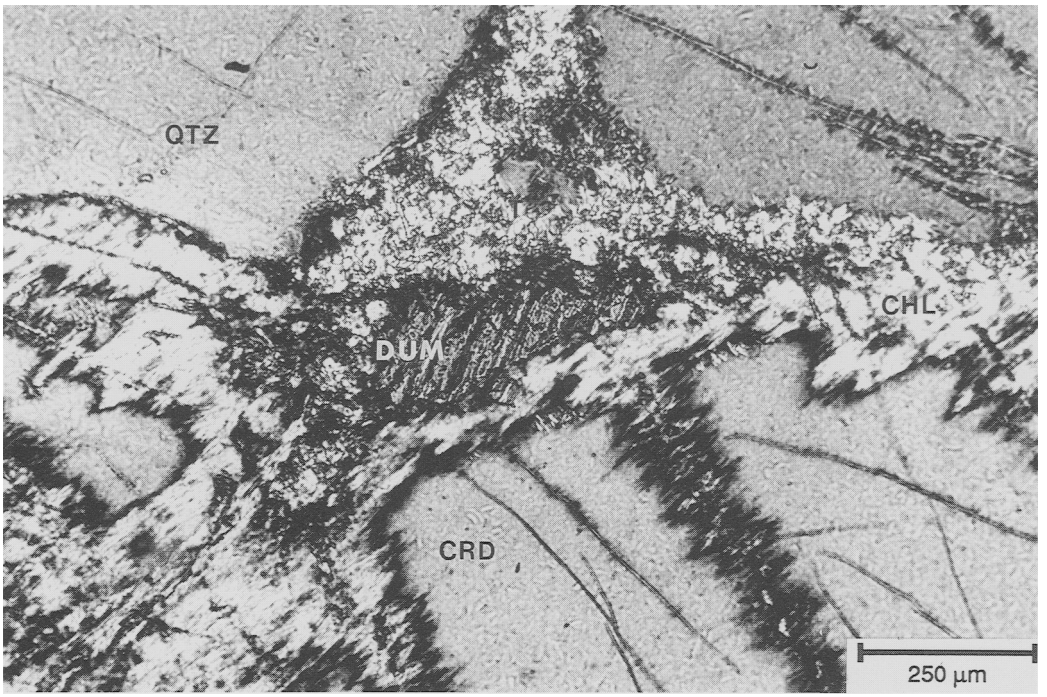

FIG. 3. Photomicrograph with crossed nicols of an alteration aggregate in cordierite (CRD) from sample AK 034. Type I dumortierite (DUM) is intergrown with chlorite, muscovite and pinite.

with the di- (Mg, Ca, Fe^{2+}) and tetravalent (Ti) substituents for octahedral Al and trivalent substituents (Al) for tetrahedral Si (see also Werding and Schreyer, 1990). The assumption of 0.75 OH per formula unit in our calculations, although the average oxide total including boron and water is 100.24% (n = 36, σ_n = 1.30), will therefore only be a rough estimate. Recent analytical data on the boron content of natural (Kayupova and Tilepov, 1977) and synthetic dumortierite (Werding and Schreyer, 1988, 1990) are generally supportive of full occupation of the B-site by boron.

Dumortierite grains were analysed from samples MA 822 (Type I, 3 grains, 5 analyses), DV 030 (Type II dumortierite, 3 grains, 8 analyses) and MA 780 (Type III, 5 grains, 23 analyses). Representative compositions of the dumortierites and associated minerals are presented in Table 2*a–c*.

Dumortierite

All three types are magnesium varieties (2.23–3.42 wt.% MgO) with variable but sometimes high iron (0.00–1.08 wt.% Fe_2O_3) and low to intermediate TiO_2 contents (0.00–2.05 wt.%). The Bamble dumortierites record the highest MgO content to date for this mineral (1.36 wt.% MgO has been reported by Vrána, 1979). Individual dumortierite grains from the three localities show no zoning, but notably TiO_2, Al_2O_3 and MgO vary from grain to grain in the same sample and between the different textural types. Titanium is low in type II dumortierite (0.00–0.46 wt.% TiO_2) and type I and III dumortierite grains not associated with respectively titaniferous magnetite and ilmenite/rutile. Moderate values (1.11–2.05 wt.% TiO_2) are obtained in type I and III dumortierites associated with the Ti-bearing phases.

Our analyses show most of the tetrahedral sites [Si(1,2)] to be slightly deficient in silicon. Al is the most likely substituent for Si at the tetrahedral sites (Fig. 6*a*). More important substitutions are implied by the very low Al-values (6.259–6.601) of the dumortierites. A high correlation between Al^{VI} and Ti, Al^{VI} and Mg (r = −0.91; r = −0.86 respectively) and a strong correlation between Ti and Mg (r = 0.72) indicate the predominant Mg + Ti = 2 Al^{VI} coupled substitution (see Fig. 6*b–c*). Subtracting the effects of this substitution, that is,

adding the total amount of Ti and an equal amount of the coupled Mg to Al^{VI} (labelled Al^{VI}*) and subtracting the total amount of Ti from Mg (labelled Mg*), reveals a strong negative correlation ($r = -0.71$) between Al^{VI}* and Mg* (Fig. 6*d*) and no significant correlation of Mg* with other elements. This indicates the introduction of Mg at the octahedral sites by the possible substitutions $3Mg = 2Al^{VI}$ and $Mg + H = Al^{VI}$.

Data on the oxidation state of Fe in dumortierite are scarce. The only two wet chemical analyses which include FeO and Fe_2O_3 (Claringbull and Hey, 1958) show that both trivalent and divalent Fe may be present. The weak inverse relation of Fe with Al^{VI} in type I and II dumortierites may suggest a low $Fe^{2+}/(Fe^{2+} + Fe^{3+})$ ratio due to substitution of most Fe as Fe^{3+} for Al^{3+} at the octahedral sites, but the substitution $Fe^{2+} + H^{+} = Al^{3+}$ would also be possible. Type III dumortierites (excluding one iron-free grain) however show a high positive correlation of Fe with Si ($r = 0.88$, Fig. 7*a*) and Mg ($r = 0.60$), strong negative with Al^{IV} ($r = -0.87$) and Al^{VI} ($r = -0.69$, Fig. 7*b*) and a weak correlation of Mg with Si ($r = 0.40$) and Al^{IV} ($r = -0.39$). This essentially involves Fe as Fe^{2+} in the Fe^{2+}, (Mg) + Si = Al^{IV} + Al^{VI}, tschermakite substitution, suggesting relatively high $Fe^{2+}/(Fe^{2+} + Fe^{3+})$ ratios.

Cordierite

The cordierite from sample MA 822, associated with type I dumortierites, is chemically unzoned and Mg-rich [$X_{Mg} = Mg/(Mg + Fe^{2+}) = 0.95$] with trace amounts of Na. Cordierite is able to incorporate important gas species such as H_2O and CO_2 in its channels. The wet chemical analyses show relatively high H_2O contents of 1.96 wt.% [$n(H_2O) = 0.67$ moles H_2O per formula unit] and very low CO_2 contents of 0.17 wt.% [$n(CO_2) = 0.025$]. The optically unzoned cordierites have optic angles between 79 and 92° with an average of 84°; γ–α ranges from 0.0075 to 0.009. Application of the triangular diagram constructed by Armbruster *et al.* (1982, p. 265) to explain the influence of H_2O and CO_2 on optical properties like birefringence and optic angle of cordierite, likewise shows that cordierite is systematically CO_2-poor with an average $n(H_2O)$ of about 0.065. The content differs from the wet chemical determination in that much lower values are recorded [$n(H_2O) = 0.33$–0.38]. The H_2O

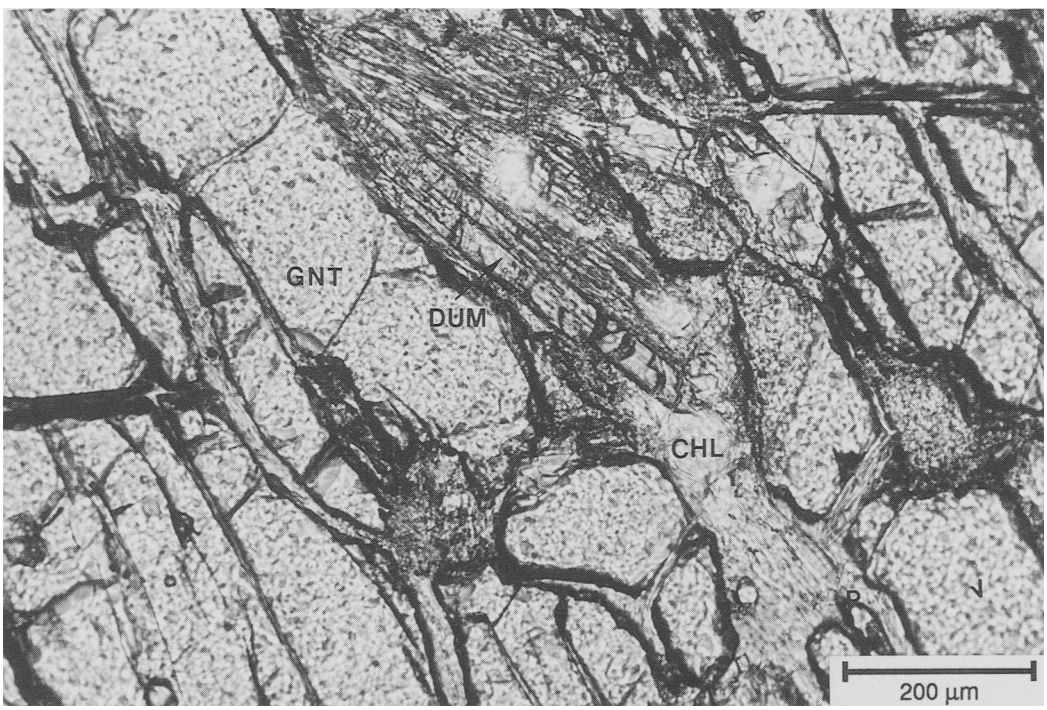

FIG. 4. Photomicrograph of type II dumortierite fibres (DUM) intergrown with chlorite (CHL) and muscovite along cracks in garnet (GNT) blasts of sample DV 030.

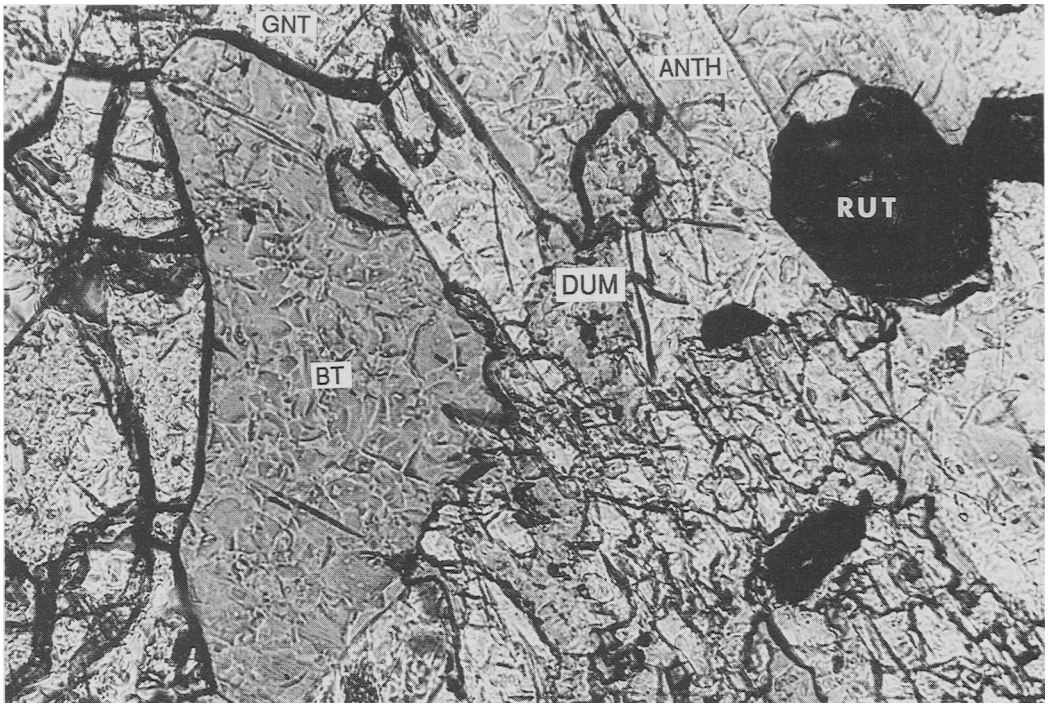

FIG. 5. Photomicrograph of irregular shaped type III dumortierite (DUM) patches replacing anthophyllite (ANTH) in sample MA 780.

content is overestimated by the wet chemical methods, mostly likely due to intergrowth of chlorite/muscovite in the analysed cordierite fraction. The optically determined H_2O and CO_2 contents correspond to a molar ratio X_{CO_2} [CO_2/(CO_2 + H_2O)] of 0.155. The same molar ratio in cordierites is, according to Johannes and Schreyer (1981), indicative of the ratio of these species in the coexisting fluid system. Utilising their experimental data in the system Mg–cordierite–H_2O–CO_2 at P_{fluid} = 5 kbar and T = 600 °C, X_{CO_2} of 0.155 in the analysed Mg-rich early M_4 vein-cordierite of sample MA 822 implies an X_{CO2} for the fluid phase of 30–40%.

Garnet

The large garnet blasts in sample DV 030 show homogeneous pyrope-rich cores with an average X_{Mg} of 0.470. Towards the retrograde cracks garnet shows a sharp but continuous decrease of Mg and an increase of Fe and Mn. X_{Mg} varies from 0.470 to 0.293; the spessartine component ranges from 1 mol.% in the core to 2 mol.% along the cracks. The grossular component is in the range 5–7 mol.%, showing no relation to the zoning in Mg, Fe and Mn.

Orthoamphibole

The structural formula of the orthoamphiboles in sample MA 780, which are partly consumed by type III dumortierite, have been normalised to 15 cations. K and Na are excluded and assigned to the A-site. Negligible amounts of Fe^{3+} are suggested by calculations from stoichiometry (Robinson *et al.*, 1982). The anthophyllites are slightly zoned with Al^{IV} (0.18 to 0.60), Al^{VI} (0.25–0.47), Mg (4.43–4.69) and Na(A) (0.06–0.15) decreasing and Si and Fe (1.90–2.22) increasing towards the orthoamphibole–dumortierite contact.

Typically the compositional variation of orthoamphiboles shows three main types of substitution: $FeMg_{-1}$, $Na(A) + Al^{IV} = \square + Si^{IV}$, and $Mg + Si^{IV} = Al^{VI} + Al^{IV}$. The anthophyllites of sample MA 780 deviate from this scheme, to the effect that Fe^{2+} shows a moderate strong negative correlation with Al^{IV}, Al^{VI} and Na(A). This suggests that the tschermakite coupled substitution essentially involves Fe^{2+} instead of Mg. The

orthoamphiboles further contain low to negligible amounts of TiO_2, MnO, CaO and K_2O.

Kornerupine

The kornerupine formula was calculated on the basis of 21.5 oxygens or 21O + (OH, F, Cl) after Moore and Araki (1979). The unzoned kornerupines with X_{Mg} ranging from 0.75 to 0.82 are relatively Al-poor with compositions close to $4(Mg,Fe)O:3Al_2O_3:4SiO_2$ (4:3:4) and slightly more siliceous than the join between the 1:1:1 and 4:3:4 compositions. The low electron-probe totals of 95.2 to 97.6 wt.% indicate high water and boron contents. Na, Ca, Mn and Ti occur in trace amounts which together total less than 0.3 wt.%.

Tourmaline

The small yellow–green tourmalines intergrown with chlorite, kyanite and quartz and the large brown–green tourmaline intergrown with vein-quartz in sample MA 822 show very similar compositional ranges. Both types of tourmaline and the large yellow tourmalines from sample MA 780 are unzoned dravites with X_{Mg} of 0.75–0.76 and 0.80–0.85 respectively. The Na/(Ca + Na) ratios are variable from grain to grain and within a grain in both samples and range 0.77–0.89 in MA 822 and 0.33–0.63 in MA 780. The high TiO_2 contents (0.50–1.68 wt.% in MA 780 and 0.49–0.69 wt.% in MA 822) are comparable to those reported from rock types containing a Ti-saturating phase (Abraham *et al.*, 1972; Henry and Guidotti, 1985).

Chlorite

The chlorites associated with type I (MA 822) and type II (DV 030) dumortierites are Al-rich clinochlores with X_{Mg} of 0.91 and 0.81 respectively.

Kyanite

Analyses of kyanite, which accompanies chlorite and quartz in cordierite replacement aggregates, show moderate to high amounts of Fe_2O_3 (0.59–1.20 wt.%).

Discussion

The textures in the investigated samples indicate that the Bamble dumortierites exclusively occur as and together with retrograde alteration products of M_3 and early M_4 assemblages in orthoamphibole–cordierite-bearing rocks.

Type I dumortierites occur intergrown with alteration products of cordierite such as chlorite, quartz and pinite. In these textures dumortierite occurs instead of kyanite and/or andalusite suggesting

$$\text{cordierite} + \text{vapour}\ (B_2O_3 + H_2O) = \text{chlorite} + \text{dumortierite} + \text{quartz}. \quad (1)$$

Reaction 1 and the development of the late M_4 mineral phases andalusite and kyanite both may occur within the same decomposed Mg-rich cordierite grains in most samples indicating similar P–T conditions for both reactions. P–T conditions are estimated at pressures of 3–4 kbar and temperatures of about 500–550 °C, when based on the Al-silicate polymorph transition of Holdaway (1971) and the low-temperature stability field of Mg-cordierite (Seifert and Schreyer, 1970). The absence of clear major optical heterogeneities or zoning towards alteration aggregates and grain boundaries in unaltered parts of the early M_4 vein-cordierite in sample MA 822 suggests that the exchange of cordierite with late M_4 fluids was limited to these alteration aggregates. From this it may be concluded that the X_{CO_2} of 30–40% deduced from the optical data represents the X_{CO_2} of the fluid phase during the early M_4 event. Late M_4 fluids probably have lower X_{CO_2} as indicated by the hydrous signature of the replacement zones and channels in cordierite. Type II dumortierites occur together with chlorite and quartz along retrograde cracks within garnet. The development of these dumortierites probably took place through the reaction of the form

$$\text{garnet (core)} + \text{vapour}\ (B_2O_3 + H_2O) = \text{garnet (rim)} + \text{chlorite} + \text{dumortierite} + \text{quartz}. \quad (2)$$

Temperature estimates for the rim of the garnet and coexisting cordierite and biotite in sample DV 030 are 420–510 °C and 460–530 °C respectively at a pressure of 4 kbar (Visser and Senior, 1990). Temperature estimates based upon the Fe–Mg exchange reaction between garnet–rim and chlorite (Grambling, 1990) are somewhat lower and in the range 400–470 °C at 4 kbar.

Type III dumortierites developed only by intergrowth with or decomposition of orthoamphibole. The compositional zoned orthoamphiboles essentially show a decrease of the ferrotschermakite substitution, $(Al_2Fe_{-1}Si_{-1})$ towards the newly formed dumortierite grains implying:

$$\text{orthoamphibole} + \text{Fe-tschermakite (Oam)} + \text{vapour}\ (B_2O_3 \pm H_2O) = \text{dumortierite}. \quad (3)$$

The P–T conditions during the development of

Table 2a. Representative analyses of dumortierite, tourmaline, cordierite, chlorite and kyanite from sample MA 822.

Mineral	Dumortierite		Trm	Crd	Chl	Ky
Spot	45	48	MA 1	51	50	53
SiO_2	30.90	30.31	36.92	49.73	28.05	36.83
TiO_2	1.11	0.46	0.59	0.00	0.00	0.00
Al_2O_3	57.24	58.42	30.88	33.42	23.72	62.54
Fe_2O_3(T)	0.44	0.00	-	-	-	1.00
FeO(T)	-	-	5.64	1.18	4.99	-
MgO	2.92	2.55	9.58	12.86	29.35	0.00
CaO	0.00	0.00	0.77	0.00	0.00	0.00
Na_2O	0.00	0.00	2.65	0.26	0.00	0.00
K_2O	0.00	0.00	0.08	0.00	0.00	0.00
B_2O_3	6.09*	6.05*	10.77*	-	-	-
H_2O	1.18*	1.17*	3.71*	(1.96)	-	-
CO_2	-	-	-	(0.17)	-	-
Cl	0.00	0.00	0.00	0.00	0.04	0.00
Total	99.88	98.96	101.59	99.58	86.16	100.37
O-Basis	18	18	31	18	28	5
Si	2.939	2.902	5.960	5.002	5.381	0.993
Ti	0.079	0.033	0.072	0.000	0.000	0.000
Al^{IV}	0.061	0.098	0.040	0.998	2.619	0.000
Al^{VI}	6.357	6.496	5.836	2.964	2.744	1.988
Fe^{3+}	0.031	0.000	-	-	-	0.020
Fe^{2+}	-	-	0.761	0.099	0.801	-
Mg	0.414	0.364	2.305	1.928	8.393	0.000
Ca	0.000	0.000	0.133	0.000	0.000	0.000
Na	0.000	0.000	0.829	0.025	0.000	0.000
K	0.000	0.000	0.016	0.000	0.000	0.000
B	1.000	1.000	3.000	-	-	-
H	0.750	0.750	4.000	-	-	-
Cl	0.000	0.000	0.000	0.000	0.013	0.000
Total	11.632	11.643	22.952	11.016	19.951	3.001
X_{mg}	-	-	0.752	0.951	0.913	-

Mn, F, Cr, Sc, Ba and Zn not detected

* - H_2O and B_2O_3 calculated assuming one B and 0.75 (OH) per formula unit for dumortierite, after Moore & Araki (1978), and 3 B and 4 (OH) per formula unit for tourmaline.
H_2O and CO_2 in cordierite determined by wet chemical methods on mineral separates.

Table 2b. Representative analyses of dumortierite, chlorite and garnet from sample DV 030.

Mineral	Dumortierite		Chl	Grt core	Grt rim
Spot	186	187	198	196	GF
SiO_2	31.62	30.79	26.70	39.92	38.63
TiO_2	0.46	0.37	0.00	0.00	0.00
Al_2O_3	58.13	58.28	24.18	22.44	21.99
Fe_2O_3(T)	0.49	0.77	-	-	-
FeO(T)	-	-	10.23	24.14	31.42
MnO	0.00	0.00	0.00	0.58	0.82
MgO	2.37	3.42	25.72	11.32	6.57
CaO	0.00	0.00	0.00	2.46	1.90
B_2O_3	6.13*	6.15*	-	-	-
H_2O	1.19*	1.19*	-	-	-
Total	100.39	100.95	86.82	100.86	100.33
O-Basis	18	18	28	12	12
Si	2.985	2.901	5.226	3.000	2.991
Ti	0.033	0.025	0.000	0.000	0.000
Al^{IV}	0.015	0.099	2.774	0.000	0.009
Al^{VI}	6.454	6.375	2.805	1.987	1.998
Fe^{3+}	0.035	0.055	-	-	-
Fe^{2+}	-	-	1.675	1.517	2.035
Mn	0.000	0.000	0.000	0.037	0.054
Mg	0.334	0.480	7.505	1.268	0.759
Ca	0.000	0.000	0.000	0.198	0.157
B	1.000	1.000	-	-	-
H	0.750	0.750	-	-	-
Total	11.606	11.685	19.985	8.007	8.003
X_{mg}	-	-	0.818	0.456	0.272

Na, K, Cl, F, Cr, Sc, Ba and Zn not detected

Table 2c. Representative analyses of dumortierite, kornerupine, tourmaline and anthophyllite from sample MA 780.

Mineral	Dumortierite		Krn	Trm	Anth#
Spot	157	151	176	TBA	KAA
SiO_2	31.42	31.30	30.87	34.84	51.61
TiO_2	1.78	1.58	0.00	1.68	0.13
Al_2O_3	57.43	56.95	41.27	30.41	4.68
Fe_2O_3(T)	0.48	0.00	-	-	-
FeO(T)	-	-	7.16	3.66	16.27
MnO	0.00	0.00	0.00	0.00	0.04
MgO	3.23	2.99	16.52	9.52	21.38
CaO	0.00	0.00	0.00	2.60	0.53
Na_2O	0.00	0.00	0.00	1.30	0.42
K_2O	0.00	0.00	0.00	0.01	0.00
B_2O_3	6.19*	6.11*	-	10.45*	-
H_2O	1.20*	1.19*	-	3.60*	-
Total	101.73	100.12	95.87	98.07	95.06
O-Basis	18	18	21.5	31	23
Si	2.939	2.967	4.015	5.795	7.494
Ti	0.125	0.113	0.000	0.210	0.014
Al^{IV}	0.061	0.033	-	0.205	0.506
Al^{VI}	6.270	6.330	6.326	5.758	0.295
Fe^{3+}	0.033	0.000	-	-	0.065
Fe^{2+}	-	-	0.779	0.509	1.911
Mn	0.000	0.000	0.000	0.000	0.005
Mg	0.450	0.422	3.203	2.361	4.628
Ca	0.000	0.000	0.000	0.464	0.082
Na	0.000	0.000	0.000	0.420	0.118
K	0.000	0.000	0.000	0.002	0.000
B	1.000	1.000	-	3.000	-
H	0.750	0.750	-	4.000	-
Total	11.629	11.615	14.323	22.724	15.118
X_{mg}	-	-	0.804	0.823	0.718

Cl, F, Cr, Sc, Ba and Zn not detected

- Fe^{3+} calculated from stoichiometry (Robinson et al., 1982).

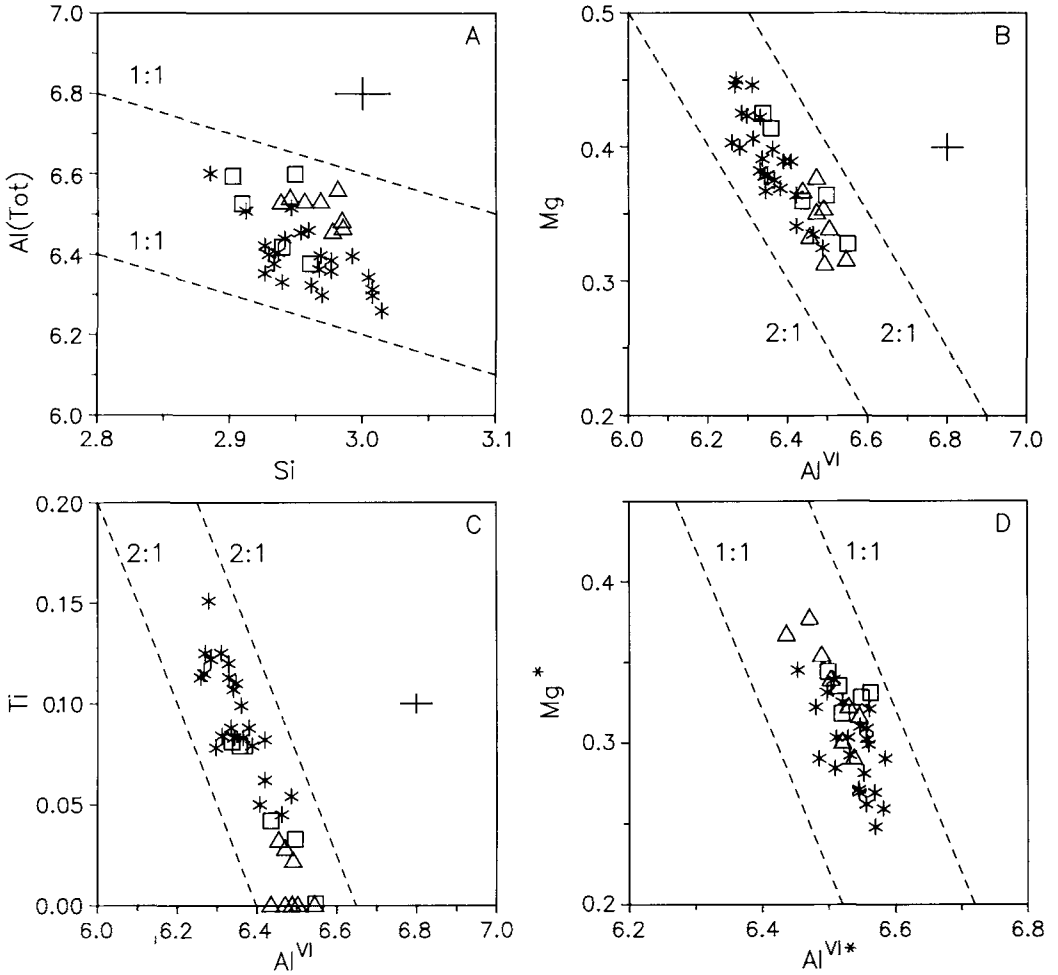

FIG. 6*a–d*. Plots of (*a*) Si versus Al(Tot), (*b*) Al^{VI} versus Mg, (*c*) Al^{VI} versus Ti, and (*d*) Al^{VI}* versus Mg* in type I (sample MA 822, triangles), type II (DV 030, squares) and type III (MA 780, asterics) dumortierites. Dashed lines show 1:1 or 2:1 ratios. Error bars are typical 1σ counting-statistics errors.

type III dumortierite cannot be estimated accurately, but the associated pinitisation of cordierite, chloritisation of biotite and growth of muscovite in garnet-cracks in the same alteration zones may suggest that hydrothermal conditions are comparable with those during the formation of type I and II dumortierites.

Titanium concentration in type I and III dumortierites depends on the presence of phases like rutile, ilmenite and titaniferous magnetite. These minerals must have acted as the major source of TiO_2 for dumortierite in reactions 1 and 3. Minor TiO_2 could have been supplied by orthoamphibole. Ti-rich dumortierites reported from the literature generally occur likewise associated with Ti-bearing phases (e.g. Beukes *et al.*, 1987; Vrána, 1979), while dumortierites intergrown with Ti-poor phases as e.g. corundum (Schreyer *et al.*, 1975) or plagioclase and quartz (Takahata and Uchiyama, 1985), show low titanium concentrations.

Oxygen fugacity levels must have been low in sample MA 780 during the dumortierite formation as suggested by the presence of Fe^{2+} in type III dumortierites. This is consistent with a very high $Fe^{2+}/(Fe^{2+} + Fe^{3+})$ ratio of the whole rock and the persistence of primary graphite in the alteration zones. Relatively higher oxygen fugacity levels are suggested during the formation of type I dumortierites from sample MA 822 on the basis of the moderately high Fe_2O_3 contents (0.69–1.20 wt.%) of kyanite grains not associated

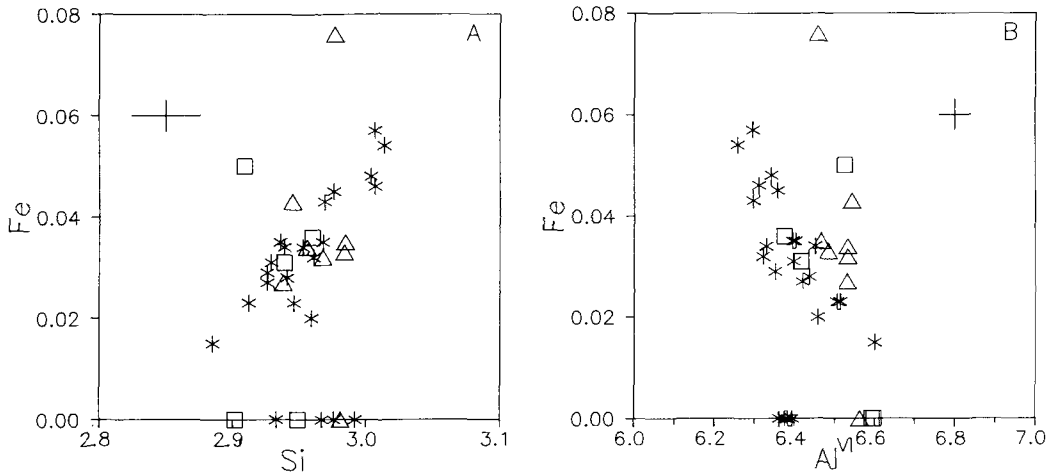

FIG. 7*a–b*. Plots of (*a*) Si versus Fe and (*b*) Al^{VI} versus Fe. Symbols as in Fig. 6*a–d*.

with titaniferous magnetite. According to Grew (1980) and Feenstra (1985), these values are characteristic of moderately to highly oxidised rocktypes.

Dumortierite-producing reactions (1–3) and associated formation of M_4 assemblages require the addition of fluid components. In 60% of the investigated samples dumortierite is accompanied by tourmaline or kornerupine, which might have acted as a source of boron for the dumortierite formation. However, textural relationships between the three minerals are lacking. Kornerupine breakdown only produces chlorite and fine-grained micas, while tourmaline grains are not observed to decompose. In fact, tourmalines from some tourmaline-bearing samples are likewise associated with the breakdown products of M_3 and early M_4 assemblages. It is therefore considered very likely that the boron oxide component in the fluid was generated outside the immediate rock volume rather than from inside. Only in sample MA 780, the breakdown of boron-bearing precursors like kornerupine might have supplied the boron for the dumortierite formation. Possible sources of boron are the late-stage K-feldspar–quartz veins and often tourmaline-bearing granitic pegmatites, which are present and sometimes abundant at most localities. The ubiquitous presence of pinite replacements in cordierite and fine grained muscovite in cracks of the garnet suggests that K, and probably other alkalis, were also available in the fluid phase.

Higher B_2O_3/H_2O ratios in the alteration fluid stabilise dumortierite relative to kyanite/andalusite together with chlorite and quartz. The presence of both dumortierite and the aluminosilicates in alteration aggregates of the same cordierite grain indicate, however, that B_2O_3/H_2O-ratios in the fluid are not uniform and vary on thin section scale. As the chemical environment for the components (FeO,MgO), SiO_2 and Al_2O_3 is very similar for both dumortierite and late M_4 tourmaline, the development of late M_4 tourmaline instead of dumortierite will mainly depend on the local availability of alkalis, notably higher Na^+ and Ca^{2+} (see mineral chemistry), higher B_2O_3 and high H_2O in the host rock and the fluid phase.

It should be realised that late M_4 overprint mainly is restricted to rock types which re-equilibrated under local rather than pervasive hydrothermal conditions. Pressure–temperature conditions for the formation of type I, II and possibly type III dumortierites in most and probably all localities are thought, nevertheless, to be very similar (500 ± 50 °C, 3–4 kbar, see above), showing no large deviation on a regional scale. This implies that metamorphic conditions during retrogradation of M_3 and early M_4 assemblages and development of late M_4 assemblages in cordierite–orthoamphibole-bearing rocks, despite the local signature of the dumortierite development, are of regional importance in the Bamble Sector. The development of dumortierite in late M_4 assemblages seems to be restricted to the upper-amphibolite facies area (Fig. 1). This is probably the result of the limited metamorphic overprint during the Sveconorwegian orogeny (M_4) in the Arendal granulite facies area.

Acknowledgements

We are indebted to Rene Poorter for assistance with the microprobe analyses. Critical comments on earlier

drafts of this manuscript were provided by Cees Maijer, Timo Nijland and Theo Kloprogge. Gunnar Raade and an anonymous referee are thanked for their reviews of the manuscript. Financial support for fieldwork from the Dr. Schürmann and the Molengraaf Foundations (to D. V.) is gratefully acknowledged.

References

Abraham, K., Mielke, H., and Povondra, P. (1972) On the enrichment of tourmaline in metamorphic sediments of the Arzberg Series, W. Germany (NE-Bavaria). *Neues Jahrb. Mineral., Mh.*, 209–19.

Alexander, V. D. Griffen, D. T., and Martin, T. J. (1986) Crystal chemistry of some Fe- and Ti-poor dumortierites. *Am. Mineral.*, **71**, 786–94.

Armbruster, Th., Schreyer, W., and Hoefs, J. (1982) Very high CO_2-cordierite from Norwegian Lapland: Mineralogy, petrology, and carbon isotopes. *Contrib. Mineral. Petrol.*, **81**, 262–7.

Beukes, G. J., Slabbert, M. J., de Bruiyn, H., Botha, B. J. V., Schoch, A. E., and van der Westhuizen, W. A. (1987) Ti-dumortierite from the Keimoes area, Namaqua mobile belt, South Africa. *Neues Jahrb. Mineral., Abh.*, **157**, 303–18.

Black, P. M. (1973) Dumortierite from Karikari peninsula: a first record in New Zealand. *Mineral. Mag.*, **39**, 245.

Bugge, J. A. W. (1943) Geological and petrographical investigations in the Kongsberg–Bamble Formation. *Norges Geol. Unders.*, **160**, 150 pp.

Claringbull, G. F. and Hey, M. H. (1958) New data for dumortierite. *Mineral. Mag.*, **31**, 901–7.

Christophe-Michel-Lévy, M., Enberger, A. and Sandréa, A. (1959) Matériaux pour la minéralogie de Madgascar. II.—La Dumortiérite de Riampotsy. *Bull. Soc. fr. Minéral. Crystallogr.*, **82**, 77–9.

Feenstra, A. (1985) Metamorphism of bauxites on Naxos, Greece. Geol. Ultraiectina 39, 206 pp.

Field, D. and Clough, P. W. L. (1976) K/Rb ratios and metasomatism in metabasites from a Precambrian amphibolite–granulite transition zone. *J. Geol. Soc. London*, **132**, 277–88.

Finlay, G. I. (1907) On an occurrence of corundum and dumortierite in pegmatite in Colorado. *J. Geol.*, **15**, 479–84.

Golovastikov, N. I. (1965) The crystal structure of dumortierite. *Sov. Phys.-Dokl.*, **10**, 493–5.

Gonnard, M. F. (1881) Note sur l'existence d'une espèce minérale nouvelle, la dumortiérite dans le gneiss de Beaunan, au-dessus des anciens aqueducs gallo-romains de la vallée de l'Izeron (Rhone). *Bull. Soc. Minéral. Fr.*, **4**, 2–8.

Graham, C. E. and Robertson, F. (1951) A new dumortierite locality from Montana. *Am. Mineral.*, **36**, 916–7.

Grambling, J. A. (1990) Internally-consistent geothermometry and H_2O barometry in metamorphic rocks: the example garnet–chlorite–quartz. *Contrib. Mineral. Petrol.*, **105**, 617–28.

Grew, E. S. (1980) Sillimanite and ilmenite from high-grade metamorphic rocks of Antarctica and other areas. *J. Petrol.*, **21**, 39–68.

Henry, D. J. and Guidotti, C. V. (1985) Tourmaline as a petrogenetic indicator mineral: an example from the staurolite-grade metapelites of NW Maine. *Am. Mineral.*, **70**, 1–15.

Holdaway, M. I. (1971) Stability of andalusite and the aluminium silicate phase diagram. *Am. J. Sci.*, **271**, 97–131.

Huijsmans, J. P. P., Barton, M., and van Bergen, M. J. (1982) A pegmatite containing Fe-rich grandidierite, Ti-rich dumortierite and tourmaline from the Precambrian, high-grade metamorphic complex of Rogaland, S.W. Norway. *Neues Jahrb. Mineral., Abh.*, **143**, 249–61.

Johannes, W. and Schreyer, W. (1981) Experimental introduction of CO_2 and H_2O into Mg-cordierite. *Am. J. Sci.*, **281**, 299–317.

Kayupova, M. M. and Tilepov, Z. T. (1977) First find of dumortierite concretions. *Acad. Sci. USSR, Dokl., Earth Sci., Sect.*, **235**, 121–4.

Kerr, P. F. and Jenney, P. (1935) The dumortierite–andalusite mineralisation at Oreana, Nevada. *Econ. Geol.*, **30**, 287–300.

Kretz, R. (1983) Symbols for rock-forming minerals. *Am. Mineral.*, **68**, 227–79.

Lamb, R. C. (1981) *Geochemical studies in Proterozoic high-grade gneiss terrain, Bamble Sector, south Norway.* Unpubl. Ph.D. Thesis, University of Nottingham.

—— Smalley, P. C., and Field, D. (1986) *P–T* conditions for the Arendal granulites, southern Norway: implications for the roles of P, T and CO_2 in deep crustal LILE-depletion. *J. Metam. Geol.*, **4**, 143–60.

Moore, P. B. and Araki, T. (1978) Dumortierite, $Si_3B[Al_{6.75}\square_{0.25}O_{17.25}(OH)_{0.75}]$: a detailed structure analysis. *Neues Jahrb. Mineral., Abh.*, **132**, 231–41.

———— (1979) Kornerupine: a detailed crystal–chemical study. Ibid. **134**, 317–36.

Nijland, T. G. and Senior, A. (1991) Sveconorwegian granulite facies metamorphism of polyphase migmatites and basic dikes, south Norway. *J. Geol.*, **99**, 515–25.

Robinson, P., Spear, F. S., Schumacher, J. C., Laird, Jo, Klein, C., Evans, B. W., and Doolan, B. L. (1982) Phase relations of metamorphic amphiboles: Natural occurrence and theory. In *Amphiboles: Petrology and experimental phase relations.* (Veblen, D. R. and Ribbe, P. H., eds.) *Rev. Mineral.*, **9b**, 1–227.

Sabzehei, M. (1971) Dumortierite from Iran: a first record. *Mineral. Mag.*, **38**, 526–7.

Schaller, W. T. (1905) Dumortierite. *Am. J. Sci.*, **19**, 211–24.

Schreyer, W., Abraham, K. and Behr, H. J. (1975) Sapphirine and associated minerals from the kornerupine rock of Waldheim, Saxony. *Neues Jahrb. Mineral., Abh.*, **126**, 1–27.

Seifert, F. and Schreyer, W. (1970) Lower temperature stability limit of Mg-cordierite in the range 1–7 kb water pressure: A redetermination. *Contrib. Mineral. Petrol.*, **27**, 225–38.

Starmer, I. C. (1985) The evolution of the south Norwegian Proterozoic as revealed by the major and mega-tectonics of the Kongsberg and Bamble

Sectors. In *The Deep Proterozoic Crust in the North Atlantic Provinces* (Tobi, A. C. and Touret, J., eds.) NATO ASI series C 158 Reidel, Dordrecht, 259–91.

—— (1990) Rb–Sr systematics of a Gardar-age layered alkaline monzonite suite in southern Norway: a discussion. *J. Geol.*, **98**, 119–23.

Takahata, H. and Uchiyama, K. (1985) Dumortierite-bearing argillaceous gneisses from the Abukuma metamorphic terrain, northeast Japan. *J. Fac. Sci., Hokkaido Univ.*, Ser. IV, **21**, 465–81.

Touret, J. (1979) Les roches à tourmaline-cordiérite-disthène de Bjordammen (Norvège méridionale) sont-elles liées a d'anciennes évaporites? *Sci. Terre,* **23**, 95–7.

Visser, D. and Senior, A. (1990) Aluminous reaction textures in orthoamphibole-bearing rocks: the pressure–temperature evolution of the high-grade Proterozoic of the Bamble Sector, south Norway. *J. Metam. Geol.*, **8**, 231–46.

—— Maijer, C., and Senior, A. (1990) Retrograde talc–kyanite–quartz assemblage from Bjordammen, Bamble Sector, south Norway. *Abs. 19th Nordic Geol. Winter Meet., Geonytt,* **17**, 119.

Vrána, S. (1979) A polymetamorphic assemblage of grandidierite, kornerupine, Ti-rich dumortierite, tourmaline, sillimanite and garnet. *Neues Jahrb. Mineral., Mh.*, 22–33.

Werding, G. and Schreyer, W. (1988) Synthetic dumortierites: Their *PTX*-dependent compositional variations in the system Al_2O_3–SiO_2–B_2O_3–H_2O. *Fortschr. Mineral.*, **66**, Beih. 1, 168.

—— —— (1990) Synthetic dumortierite: its *PTX*-dependent compositional variations in the system Al_2O_3–B_2O_3–SiO_2–H_2O. *Contrib. Mineral. Petrol.*, **105**, 11–24.

[*Manuscript received 15 June 1990; revised 4 January 1991*]